Segrest, J. P., Gulik-Kryzwicki, T., & Sardet, C. (1974) *Proc. Natl. Acad. Sci. U.S.A. 71*, 3294–3298.
Segrest, J. P., & Kohn, L. D. (1973) in *Protides of the Biological Fluids–21st Colloquium* (Peeters, H., Ed.) pp 183–189, Pergamon Press, New York.
Silverberg, M., Furthmayr, H., & Marchesi, V. T. (1976) *Biochemistry 15*, 1448–1454.
Tomita, M., & Marchesi, V. T. (1975) *Proc. Natl. Acad. Sci. U.S.A. 72*, 2964–2968.
Warren, L. (1959) *J. Biol. Chem. 234*, 1971–1975.

Transient Electric Dichroism Studies of the Structure of the DNA Complex with Intercalated Drugs†

M. Hogan, N. Dattagupta, and D. M. Crothers*

ABSTRACT: We describe electric dichroism, fluorescence electric dichroism, and equilibrium binding studies whose purpose is to examine the structure of the complex between DNA and intercalating drugs (ethidium bromide, actinomycin D, 9-aminoacridine, and proflavin). We show that the DNA length increase which results from intercalation is not always 3.4 Å per bound drug as often idealized but varies from drug to drug, the range being 2–3.7 Å. From the limiting dichroism at high fields we calculate that the drugs are not perpendicular to the helix axis when intercalated but are tilted from perpendicularity by 21 ± 7° along their long axis. We propose that tilting occurs because base pairs neighboring the intercalated drug are flattened by the heterocycle and are therefore incompatible with adjacent propeller-twisted base pairs. We show that DNA is not bent or kinked by intercalators; therefore a conformational change must occur which compensates for the tilt of the complex. Others have suggested that 5′ pyrimidine 3′–5′ purine is the preferred sequence for intercalation. We propose that the conformational change which compensates for the tilt of the complex reflects the twofold rotational symmetry of the binding site, thereby maintaining the linearity of the helix. The magnitude of the conformational change required suggests that, as a result of intercalation, stacking is reduced between the 5′ pyrimidine and its 5′ neighbor.

Although the concept of intercalation was first proposed by Lerman 17 years ago (Lerman et al., 1961) and has been widely used as a model for ligand binding, the detailed structure of the intercalated complex in DNA is not known. Crystal structures have been solved at 3-Å resolution for ethidium bromide (Jain et al., 1977; Tsai et al., 1977), actinomycin (Sobell & Jain, 1972), proflavin (Neidel et al., 1977; Seshadri et al., 1977), and 9-aminoacridine (Sakore et al., 1977) complexes with nucleotides and dinucleotide helices. Such structures provide valuable information concerning local drug–nucleic acid interactions, but problems may arise when extending the models to long segments of DNA helix (Alden & Arnott, 1977).

So far, the structure of the intercalated complex in large DNAs has been impossible to measure at atomic resolution. However, as we have shown in previous papers (Hogan et al., 1978; Dattagupta et al., 1978; Crothers et al., 1978; Klevan et al., 1978), electric dichroism techniques can be used to measure the orientation of chromophores and the DNA length and conformation changes which result from ligand and protein binding. In combination, this information can put rigorous limits on the range of possible intercalated structures.

Here we report dichroism studies on the binding of several intercalators to DNA. Based upon these measurements we propose that, when intercalated, drugs are tilted by at least 20° along the long base-pair axis. Overall, the helix remains linear, due we believe to extensive conformational changes in the "excluded site" adjacent to the intercalator.

† From the Department of Chemistry, Yale University, New Haven, Connecticut 06520. *Received September 1, 1978.* Supported by a grant, CA 15583, from the National Cancer Institute. M.H. was supported by National Institutes of Health Training Grant GM 07223.

Dichroism Theory

Fiber diffraction data indicate that the bases in DNA form an extremely regular lattice. Therefore, when DNA is oriented in an electric field, chromophores bound to DNA will, like the bases, display linear dichroism. At any wavelength where the ligand absorbs light the reduced dichroism ρ is defined by

$$\rho = (A_{\parallel} - A_{\perp})/A \quad (1)$$

in which $A_{\parallel}$ and $A_{\perp}$ are the absorbances measured with light polarized parallel and perpendicular, respectively, to the applied electric field, and A is the absorbance in absence of the field. The dichroism due to a particular transition moment can be expressed by (Okonski et al., 1959)

$$\rho_i = \frac{3}{2}(3\cos^2\alpha_i - 1)\Phi \quad (2)$$

where α_i is the angle between the ith transition moment and the axis of orientation and Φ is the fractional orientation (Okonski et al., 1959), equal to the ratio (ρ/ρ_∞) of the measured dichroism to the dichroism at perfect orientation, achieved in the limit of infinite field. Dichroism remains constant over those wavelengths where absorbance arises from a single transition (Ding et al., 1972). Many intercalators display multiple visible and near-UV transitions and will therefore have associated with each transition a different dichroism value. From measurements at different wavelengths it is possible to measure independently the angles α_i between each of the optical transition moments and the axis of orientation.

The intense visible absorbances displayed by intercalated heterocycles arise from π–π^* transitions and are therefore directed in the aromatic plane. Several intercalators display

0006-2960/79/0418-0280$01.00/0

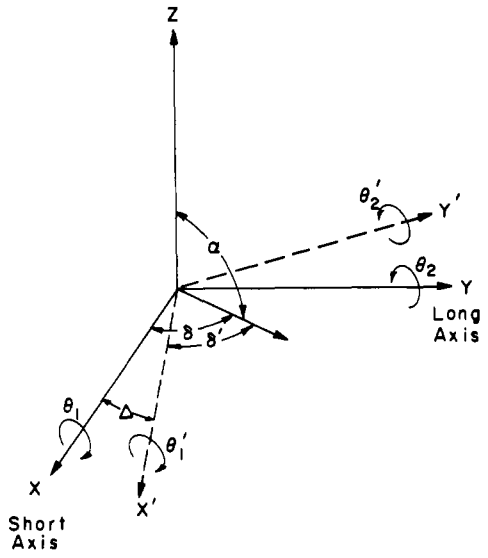

FIGURE 1: The coordinate system used to calculate the orientation of chromophores from dichroism data. X is the short axis of a chromophore; Y, the long axis. Δ is the angle by which a set of axes X' and Y' are rotated about their common Z axis perpendicular to the XY plane. The axes X' and Y' are used to define the orientation of a base pair adjacent to the chromophore and are considered further in the Results and Discussion sections. The angles θ and θ' are zero when the chromophore or base-pair planes coincide with the XY or $X'Y'$ planes. α is the angle between a transition moment and the Z axis. Notice that the XY and $X'Y'$ planes are coincident and perpendicular to the Z axis, which is the axis of orientation of the DNA molecule in the electric field.

multiple absorptions for which the direction within the heterocycle plane of the corresponding transition moment is known. If the angles α_i are measured for these transitions when the drug is bound to DNA, they can be used to specify the orientation of the heterocycle when intercalated.

The method for making this calculation is that derived by Rill (1972). Let δ_i be defined as the angle between a transition moment in a planar heterocycle and an appropriately chosen X axis (Figure 1). Next, define θ_1 as the tilt angle by which the heterocycle plane is rotated about this X axis; the twist angle θ_2 is defined as the angle of rotation of the heterocycle about a perpendicular axis Y.

The angle α_i between a vertical Z axis and the ith transition moment can be uniquely specified from the values δ_i, θ_1, and θ_2. Therefore, as has been shown by Rill (1972), the dichroism ρ_i can be expressed for π–π^* transitions in terms of δ_i, θ_1, and θ_2

$$\rho_i = \frac{9}{2}\left[(\cos\delta_i \cos\theta_1 \sin\theta_2 - \sin\delta_i \sin\theta_1)^2 - \frac{1}{3}\right]\Phi \qquad (3)$$

where the zero of tilt and twist specifies a plane perpendicular to the axis of orientation Z (Figure 1). Equation 3 can be used to calculate angles from measured dichroism values ρ_i. If δ_i are known for at least two transition moments, θ_1 and θ_2 may be solved from the simultaneous equations for ρ_i, thereby specifying the orientation of the intercalator in the helix.

Several important properties of linear dichroism can be seen from eq 3. First, when a chromophore is perpendicular to the axis of orientation, dichroism is independent of the orientation δ_i of π–π^* transitions in the heterocycle; the angle between the transition moment and the Z axis will in all cases be 90° and will give the maximum negative dichroism value of −1.5. Second, for any amount of tilt or twist there is one value δ_i that gives maximum negative dichroism. This simply means that any plane, regardless of its inclination relative to a vertical Z axis, contains one vector component that is perpendicular to Z. Therefore an intercalator could display dichroism which approaches −1.5 for one transition direction even though the molecule is tipped from the perpendicular plane.

Effects of Helix Distortions. Binding or kinking of DNA alters the symmetry of the helix, thereby changing the spacial averaging of transition moments. Random distortions of the helix make DNA more isotropic, thereby reducing dichroism values (Ding et al., 1972). Distortions which are regularly disposed along the helix will bend DNA into a superhelix. As the amount of superhelicity increases, dichroism values can approach zero and even change sign (Ding et al., 1972; Crothers et al., 1978). Therefore the extrapolated dichroism values ρ_∞ will be independent of the amount of bound ligand only if the helix remains linear.

Length Changes. As we stated earlier (Hogan et al., 1978), rodlike DNA molecules orient in an electric field as predicted for an induced-type moment (Tinoco, 1955)

$$\rho(t) = \rho(1 - e^{-t/\tau}) \qquad (4)$$

where $\tau = {}^1/_6 D_r$. For DNA, the rotational diffusion coefficient D_r is as derived by Broersma (1960) for rods

$$D_r = \frac{3kT}{\pi\eta L^3}\left(\ln\frac{L}{b} - 1.57\right) \qquad (5)$$

where L and b are respectively the DNA length and half-width.

This expression for D_r is independent of the kind of particle studied and therefore can be used to measure the length of DNA–ligand complexes. D_r is dominated by its L^3 term and is relatively insensitive to thickness changes. Therefore dichroism rise times can be used to measure length changes induced by intercalators with an accuracy equal to 1–2% of the length.

Fluorescence Dichroism. When intercalated, heterocycles generally show fluorescence changes which are attributed to the environmental effects experienced inside the helix (LePecq & Paoletti, 1967). In contrast, when these same chromophores bind ionically outside the helix, their fluorescence properties are very different (Dourlent & Helene, 1971; Weill & Calvin, 1963).

For solutions with low optical densities, the total fluorescence intensity f_0 is proportional to the absorbance at some wavelength A_λ (Turro, 1965)

$$f_0 = c_\lambda A_\lambda \qquad (6a)$$

where c_λ is proportional to the quantum yield for fluorescence. The total fluorescence displayed when the sample absorbs polarized light will therefore show the same proportionality

$$f_\parallel = c_\lambda A_\parallel \qquad (6b)$$

$$f_\perp = c_\lambda A_\perp \qquad (6c)$$

where $f_\parallel$ and $f_\perp$ are the total fluorescence displayed by the sample when absorbing polarized light of a particular wavelength λ; $f_\parallel$ and $f_\perp$ are of course equal for unoriented samples.

The fluorescence quantum yield is a molecular property that describes the probability that, once absorbed, light will be emitted as fluorescence. Therefore the proportionality c_λ is independent of the orientation of the chromophore in space. Changes in fluorescence intensity that occur when a sample orients in an electric field are hence a result of absorbance changes only. Thus using eq 6a–c we can relate the dichroism ρ to the dichroism measured by fluorescence ρ^f

$$\rho \equiv \frac{A_\parallel - A_\perp}{A_0} = \frac{c_\lambda A_\parallel - c_\lambda A_\perp}{c_\lambda A_0} = \frac{f_\parallel - f_\perp}{f_0} = \rho^f \qquad (7)$$

and by analogy with eq 2

$$\rho^f = \frac{f_{\parallel} - f_{\perp}}{f_0} = \frac{3}{2}(3\cos^2\alpha - 1)\Phi \qquad (8)$$

where, as in the case of ordinary absorbance dichroism measurements, α is the angle corresponding to the transition moment for the absorption of light. Because the actual value of c_λ never enters into the calculation, fluorescence can be monitored at any wavelength or band or wavelengths appropriate for the chromophore of interest.

If all species are bound in the same way, they will fluoresce with the same quantum efficiency. Dichroism measured by absorption ρ should then equal that measured by fluorescence ρ^f. If there exist two kinds of bound chromophores with different fluorescence properties, as has been proposed for intercalators at high r (ratio of bound ligand/base pairs) values, the averaged dichroism measured by fluorescence will be weighted more heavily toward the contribution of the stronger fluorophore. In the limit that one species is completely nonfluorescent, the measured dichroism ρ^f will measure the dichroism ρ of the fluorophore alone.

If ρ and ρ^f are measured and found to be equal, it may be concluded that there is only one kind of bound species or that, if more than one, they have the same quantum yield or the same angle α.

Materials and Methods

Calf thymus DNA (Sigma I) was sonicated and fractionated over Sepharose 4B as described previously (Hogan et al., 1978). Dichroism measurements utilized this DNA fraction after overnight dialysis against the dichroism buffer (0.5 mM Na_2HPO_4, 1 mM NaH_2PO_4, 0.25 mM Na_2EDTA, pH 7.0). DNA concentrations were determined on a Cary Model 14 spectrophotometer, using $\epsilon_{258} = 12\,900$ M^{-1} cm^{-1}, in terms of base pairs.

Intercalating drugs were purchased commercially (ethidium bromide,[1] Sigma; proflavin, Aldrich; 9-aminoacridine, Aldrich; and actinomycin D, Boehringer) and used without further purification.

Dichroism was measured on a modified temperature-jump apparatus as described previously (Hogan et al., 1978). Fluorescence dichroism was measured with the same device, using instead a cell with right-angle fluorescence detection. In all cases, total fluorescence was measured by monitoring emission through a 570-nm high-pass filter (Oriel).

Let $I_{\parallel}(E)$ be defined as the total fluorescence signal measured in the band of wavelengths above 570 nm when an oriented sample absorbs parallel polarized light, and let I_0 be the total fluorescence measured under identical conditions but before orientation. Then since

$$\rho \equiv \frac{3}{2}\frac{A_{\parallel}(E)}{A_0} \qquad (9a)$$

the fluorescence dichroism may also be defined in terms of its parallel component only.

$$\rho^f \equiv \frac{3}{2}\frac{I_{\parallel}(E)}{I_0} \qquad (9b)$$

Dichroism values ρ^f reported here were calculated using eq 9b.

[1] Abbreviations used: EB, ethidium bromide; AM, actinomycin D; PF, proflavin; 9-AA, 9-aminoacridine; 1-MePNR, 1-methylphenyl neutral red; py, pyrimidine; pu, purine.

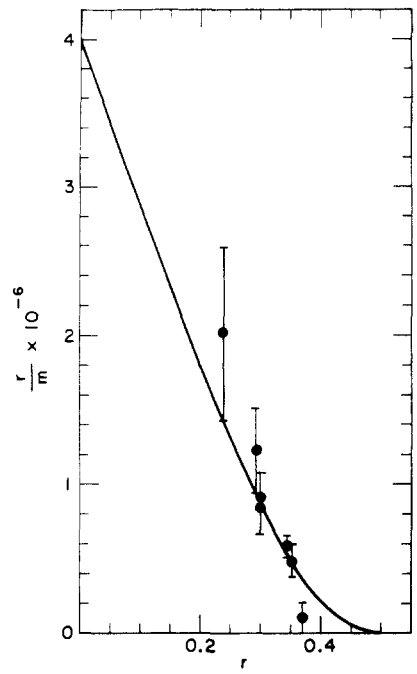

FIGURE 2: Scatchard plot of ethidium bromide binding to calf thymus DNA in dichroism buffer, 11 °C. The solid line is the isotherm predicted from the neighbor exclusion model assuming two base pairs per binding site (see text).

Equilibrium dialysis of the ethidium bromide (EB) was performed in a thermostated water bath at 11 °C, using the dichroism buffer. The total concentration of EB inside the dialysis membrane ($C_B + C_f$) was measured by absorbance at 520 nm after dissociation in $NaDodSO_4$; we used as the extinction coefficient for EB measured in the dissociation buffer $\epsilon_{520} = 6290$. The concentration of free ethidium, C_f, was determined from the absorbance of the dialysate with $\epsilon_{480} = 5850$ (Bresloff, 1974).

Binding data were plotted in the Scatchard formalism (Scatchard, 1949) r/C_f vs. r, where r is the ratio bound ligand/base pairs and C_f is the concentration of free ligand.

The data were fit to the equation for neighbor exclusion binding with n, the number of excluded base pairs, = 2 (Crothers, 1968; McGhee & Von Hippel, 1974)

$$\frac{r}{m} = K\frac{(1 - 2r)^2}{1 - r} \qquad (9)$$

where K is the intrinsic binding constant.

Results

Ethidium

Equilibrium Dialysis. In high salt buffers, at r values below 0.5, EB binding to calf thymus DNA can be explained by a single intercalated complex with a neighbor exclusion range $n = 2$ base pairs and a binding constant K which is dependent on the ionic strength of the medium (Waring, 1965). Intercalation is accompanied in high salt by a red shift of the ethidium absorbance maximum to 520 nm and a decrease in the extinction coefficient at 520 nm to 4090 M^{-1} cm^{-1} (Waring, 1965).

Figure 2 shows a Scatchard plot of EB binding to calf thymus DNA in dichroism buffer. Within experimental accuracy, the isotherm is fit by a single neighbor exclusion binding mechanism with $n = 2$ and $K = 4 \times 10^6$ M^{-1}, in good agreement with other determinations of EB binding in low salt (Weill & Calvin, 1963). The absorption maximum of bound

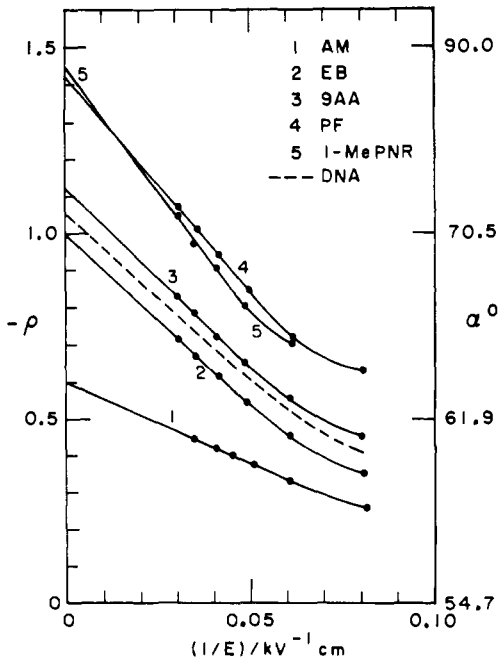

FIGURE 3: Representative field extrapolations for drug DNA complexes in dichroism buffer, 11 °C. (1) AM, 440 nm; (2) EB, 520 nm; (3) 9AA, 427 nm; (4) PF, 430 nm; (5) 1-MePNR, 530 nm.

Table I

ligands	λ (nm)	r	$-\rho_\infty$	α (deg)
EB	520	0.050	0.87	68
		0.109	1.00	71
		0.219	1.06	72
		0.373	1.06	72
PF	430	0.02	1.42	82
		0.03	1.42	82
9-AA	407	0.10	1.13	73
AM	470	0.05	0.60	63
		0.04	0.58	62
		0.28	0.35	60
1-MePNR	530	0.027	1.45	84
DNA	265		1.05	72

ethidium in dichroism buffer is 520 nm at both 0.05r and 0.2r. The extinction coefficient is also independent of r; we found 4000 ± 200 M^{-1} cm^{-1} at 520 nm.

Therefore, within the limits of experimental accuracy, ethidium bromide binding in the dichroism buffer is tighter but otherwise indistinguishable by these criteria from the binding it displays at low r values at high ionic strengths. If the mode of binding is different, the bound ethidium complex or complexes must have binding and absorbance properties very similar to the intercalated complex.

Dichroism. Figure 3 shows a plot of ethidium dichroism vs. field strength at 520 nm, representative of the data used to calculate the angles α in Table I. As seen previously (Hogan et al., 1978), dichroism values are precise and extensive orientation is achieved at the highest field strengths. The extrapolation of the measured values ρ to perfect orientation is linear and consistent with the flow model for DNA orientation (Hogan et al., 1978). The angles α were calculated from these extrapolated values using eq 2.

Ethidium dichroism shows no significant r dependence at 520 nm, giving at all degrees of saturation $\alpha = 70 \pm 2°$ (Table I). The visible absorbance band for bound ethidium centered at 520 nm has been ascribed (Houssier et al., 1974) to a transition moment oriented 30° with respect to the molecular X axis (Figure 4). According to NMR (Patel & Canuel, 1977) and crystallographic studies (Jain et al., 1977; Tsai et al., 1977), the ethidium benzene ring, and hence this visible transition moment, is directed into the DNA small groove. Because the dichroism measured at 520 nm does not vary with the amount of bound ethidium, little or no bending or kinking of the DNA helix can be occurring upon ethidium binding. The measured 70° angle therefore suggests that, when intercalated, ethidium is *not* perpendicular to the helix axis.

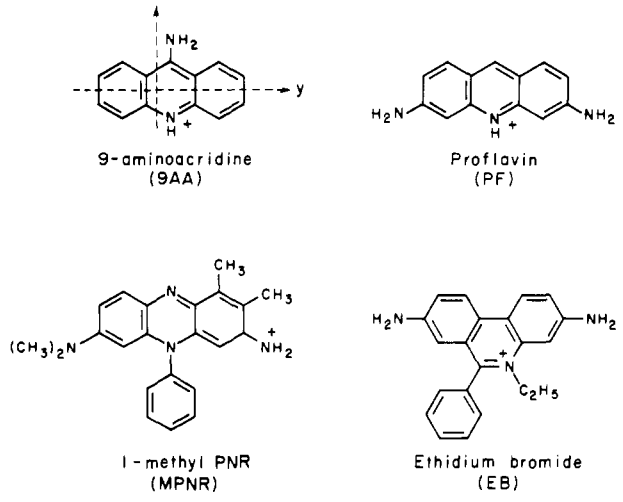

FIGURE 4: The structure of the four intercalators.

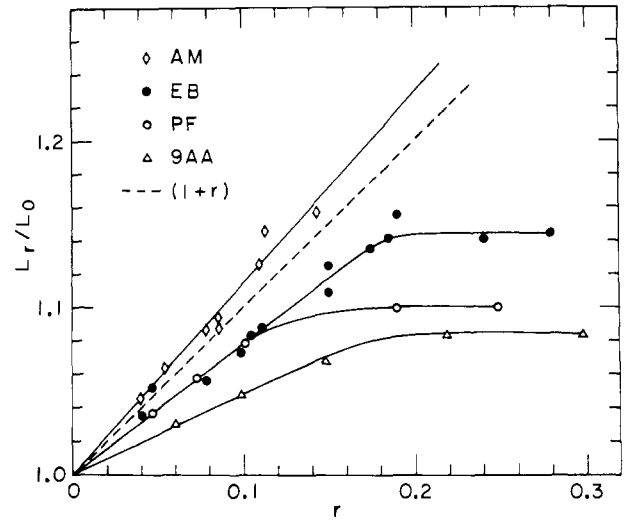

FIGURE 5: The dependence of complex length on r. The dotted line corresponds to the idealized 3.4-Å length increase per drug. (●) EB, (◊) AM, (○) PF, (△) 9AA.

The length change induced by ethidium intercalation was measured from the dichroism rise time and is shown in Figure 5. DNA length increases linearly with the degree of saturation up to about $r = 0.2$, implying, as did the binding data, that no change in binding mechanism occurs over that range of r values. The slope of the line indicates a 2.7-Å increase in DNA length per bound ethidium. This value falls slightly short of the 3.4-Å length increase often idealized for intercalators, but, as will be shown below for other drugs and has been shown elsewhere by other techniques (Cohen & Eisenberg, 1969; Zipper & Bünemann, 1975; Müller & Crothers, 1968), a 3.4-Å increase may be only an approximation.

Dichroism Spectra. Ethidium has several optical transitions available for study; in particular, the transitions at 280 and 316 nm in the bound complex are intense and directed along the molecular Y axis (Houssier et al., 1974). Simultaneous measurement of the dichroism at 316 and 520 nm defines the spacial orientation of two vectors in the ethidium plane and

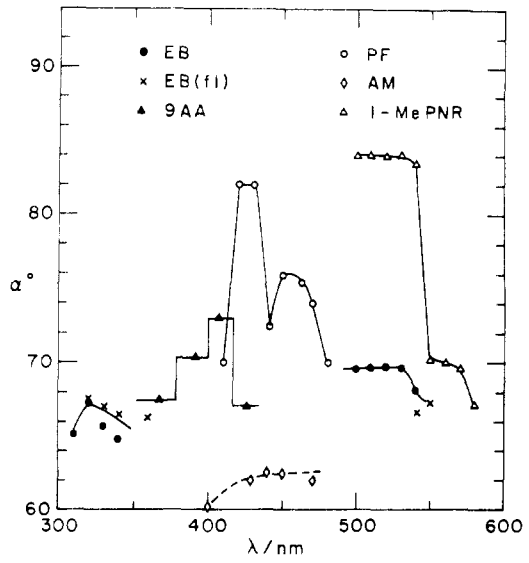

FIGURE 6: Dichroism spectra. Conditions as in Figure 2. (●) EB, (×) EB fluorescence dichroism, (○) PF, (▲) 9AA, (◇) AM, (△) 1-MePNR.

therefore the orientation of ethidium in the helix. EB dichroism in the region from 310 to 325 nm is nearly independent of λ (Figure 6) and once again implies that α is very nearly 70°.

The simplest interpretation of these results, rather surprisingly, is that when intercalated into DNA ethidium is tipped from perpendicularity along both its transition moments, yet causes no net bending or kinking of the helix axes. Impurities in the DNA, machine artifacts, or inadequacies in dichroism theory could also explain these low calculated angles for ethidium; however, several controls can be cited which make these artifacts unlikely.

First, as mentioned earlier, if the observed dichroism is in fact an average arising from ethidium intercalated perpendicular to the helix axis and some outside bound species with a transition moment more nearly parallel to the helix axis, the resulting average value for α could appear lower than 90°. Figure 6 shows the fluorescence dichroism spectrum for ethidium at $0.05r$. In low-salt buffers, at r values greater than 0.5, there occurs a second kind of ethidium binding (Lepecq & Paoletti, 1967) which is presumed to be ionic binding outside the helix (Dourlent & Helene, 1971).

This "outside-bound" form is weakly fluorescent (Lepecq & Paoletti, 1967); consequently, if the measured ethidium dichroism values ρ_i are artificially low due to contributions from this other kind of binding, the fluorescence dichroism ρ^f should be more negative than ρ, i.e., specify an angle α more nearly 90°. As seen in Figure 6, the fluorescence dichroism spectrum for ethidium is not significantly different from its absorbance dichroism spectrum, implying that the low measured values are not due to outside-bound material.

A second verification of the low ethidium values may be drawn from the very large negative dichroism values seen for individual transition moments in 1-methylphenyl neutral red (1-MePNR) and proflavin complexes with calf thymus DNA (Figure 3). Measured dichroism values which approach the theoretical limit of −1.5 at low r values preclude machine or material artifacts that cause systematically lowered values of ρ and argue that the DNA helix is rigid and rodlike.

Another direct verification of the ethidium dichroism values comes from a study of the effect of distamycin A on bound ethidium. The nature of the effect will be described in another paper (Dattagupta, Hogan, & Crothers, to be published). Here, we need only state that distamycin induces a massive, long-range conformational change in calf thymus DNA. Each bound distamycin makes available 2–3 EB binding sites where bound ethidium shows negative dichroism, at 520 nm, larger than 1.45. We conclude that the 520-nm transition in this distorted DNA is perpendicular to the helix axis, implying very strongly that in undistorted DNA it is not.

Other Intercalators

If ethidium binding is representative of intercalation in general, other recognized intercalators should show features similar to ethidium.

Actinomycin D. Actinomycin D (AM) is, along with ethidium, the most studied of the intercalating ligands (Sobell & Jain, 1972; Zipper & Bünemann, 1975; Müller & Crothers, 1968). DNA length changes and the dichroism of its 440-nm absorbance band were measured as was done for ethidium. A representative field extrapolation is shown in Figure 3 for AM; its dichroism spectrum is shown in Figure 6.

As can be seen in Table I, AM dichroism shows no r dependence, giving at all values $\alpha = 61 \pm 2°$. The AM absorbance at 440 nm is thought to correspond to a transition moment along the long molecular axis (Yamoka & Ziffer, 1968). This means that the long axis of AM is, like ethidium, tilted in the intercalated complex.

The AM-induced DNA length increase is shown in Figure 5. The length increment is linear for low r values and corresponds to a 3.7-Å increase per bound AM. This value agrees with values calculated from X-ray scattering (Zipper & Bünemann, 1975) and from viscosity and sedimentation measurements (Müller & Crothers, 1968) and implies again that only intercalation occurs at low r.

Proflavin. Figure 6 shows the dichroism spectrum for proflavin at $r = 0.033$ and 0.2. In general, acridines show several visible transitions which are directed along the long and short molecular axes (Lang & Löber, 1969; Müller, unpublished results; Ingram & Johansen, 1969; Zanker & Schmid, 1957; Wittwer & Zanker, 1959). Upon derivatization to form proflavin, these transitions merge. The composite absorption band displays an intense long-wavelength transition polarized along the proflavin long-axis Y and a weaker short-wavelength shoulder which is directed along the X axis (Wittwer & Zanker, 1959). It is predicted theoretically that there may be other weak transitions in the absorbance band with an energy very near that of the other two (Müller, unpublished results; Ingram & Johansen, 1969), but they have not been detected by standard methods.

As seen in Figure 6, the dichroism spectrum of bound proflavin has a structure which specifies at least four transitions centered at 430, 440, 450, and 480 nm. The absorption band is centered about 455 nm, so we ascribe the α angle maximum at 450 nm to the intense Y-directed transition and the maximum at 430 nm to the weaker X-directed transition.

The intrinsic dichroism of the 450-nm transition is −1.25 (Figure 3). This implies that, like EB and AM, the long axis of bound proflavin is not perpendicular to the helix axis.

The dichroism band at 430 nm displays a very high negative value, implying that the X-directed transition is nearly perpendicular to the helix axis. As will be shown later, this is also consistent with the dichroism seen for EB and AM.

The weak transitions contributing to the dichroism at 440 and 480 nm have not been observed experimentally. Therefore we cannot with certainty ascribe to these transitions a direction in bound proflavin. However, their smaller α-angle contribution suggests that these two transitions may also be directed along the long proflavin axis.

Table II

ligand	λ (nm)	Δ (deg)	δ (deg)	δ′ (deg)	calcd tilt and twist angles[g] (deg) drug θ_1	drug θ_2	complex θ_1'	complex θ_2'	dichroism calcd ρ	calcd ρ'	obsd ρ
EB	320_y	-7^a	90	83					−0.81	−0.81	−0.81
	520_x		−30	−37	23	10	24	6	−1.0	−1.0	−0.97
	320_y	-11^b	90	79					−0.81	−0.84	
	520_x		−30	−41			24	5	−1.0	−1.0	
AM	440_y	0^c	90	90	28		28		−0.58	−0.58	−0.58
9-AA	365_x		90	80					−0.86	−0.87	−0.86
	427_y	-10^d	90	80	23	17	25	16	−0.86	−0.87	−0.86
	386_x		0	−10					−1.1	−1.05	−1.1
	407_y		0	−10					−1.1	−1.05	−1.1
PF	430_x	-27^e	0	−27	14	2	15	−3	−1.49	−1.48	−1.42
	450_y		90	63					−1.24	−1.21	−1.25
	430_x	0^f	0	0	14	2	14	2	−1.45	−1.45	
	450_y		90	90					−1.24	−1.24	

[a] Jain et al., 1977. [b] Tsai et al., 1977. [c] Sobell & Jain, 1972. [d] Sakore et al., 1977. [e] Neidel et al., 1977. [f] Alden & Arnott, 1977. [g] Rill, 1972.

The proflavin-induced length change is shown in Figure 5. Deviations from linearity begin about $r = 0.2$ in these low-salt buffers, perhaps due to the appearance of outside-bound dye. At low r, the length change indicates a 2.7-Å increase per proflavin and is identical with the value measured by ultracentrifugation and viscometry in high salt (Cohen & Eisenberg, 1969).

9-Aminoacridine (9-AA) is of interest because its characteristic acridine absorbance bands are unaltered by substitution at the 9 position. As shown in Figure 6, transitions polarized along both axes are inclined to 70° in this ligand.

Acridines are known to bind outside DNA at high r values, so care was taken to define the 9-AA-length increase in the limit of low r values. At low r the length increase is linear and corresponds to 2 Å per 9-AA (Figure 5), again indicative of intercalative binding.

Calculated Orientations

Because the position of the transition moments is known with some certainity for EB, AM, 9-AA, and proflavin, eq 2 can be used to calculate the inclination of these chromophores in the helix.

Ethidium Bromide. The 520-nm transition in EB is directed toward the phenyl group ($\delta = -30$) while the 320-nm transition is directed along the Y axis ($\delta = 90$) (Houssier et al., 1974; Hudson & Jacobs, 1975). From these δ values and the measured dichroism, the title θ_1 and twist θ_2 of the heterocycle were calculated using eq 2 and are presented in Table II. As implied from the low extrapolated dichroism, bound ethidium is not perpendicular to the helix axis, the best fit to the data being an orientation with the ethidium Y axis tilted 23° and the X axis twisted 10°.

9-Aminoacridine has four transitions directed along the molecular X and Y axes (Figure 4), $\delta_{386} = \delta_{407} = 0$, $\delta_{375} = \delta_{427} = 90$ (Müller, unpublished results; Ingram & Johansen, 1969; Zanker & Schmid, 1957; Wittwer & Zanker, 1959; Zanker & Wittner, 1963). These values δ and the measured dichroism values specify values for θ_1 and θ_2 very similar to those for ethidium (Table II). The long-axis tilt is identical with that for ethidium (23°), but the complex has 7° more twist.

Actinomycin D has only one visible transition, which is directed along the molecular Y axis (Figure 4), $\delta_{440} = 90°$ (Yamoka & Ziffer, 1968). Hence only the tilt may be calculated; the value is 28°, very similar to values for EB and 9-AA (Table II).

For *proflavin*, if the 430-nm band is assigned X orientation and the 450-nm extremum Y orientation, we generate a solution of eq 2 similar to that seen for the other intercalators (Table II).

Calculating the Orientation of the Complex

There is evidence that suggests that intercalators show a preference for the sequence 5′ pyrimidine 3′–5′ purine (Jain et al., 1977; Tsai et al., 1977; Krugh & Reinhardt, 1975). X-ray diffraction data indicate that when bound to helix fragments with this sequence, the complex shows approximate twofold symmetry with bases stacked nearly parallel to the intercalator. The angular orientation of the drug and base-pair planes are identical in such a parallel complex. Therefore the orientation of the drug also specifies the orientation of that piece of DNA helix adjacent to the drug. Although the plane of the adjacent bases is parallel to that of the intercalated drug, drug and base-pair axes need not overlap. In general the drug coordinates (X, Y, and Z) can be related to a set of parallel base coordinates (X', Y', and Z) by the angle Δ between the vectors X and X' (Figure 1). The direction of any vector in the drug plane can be similarly redefined; therefore the direction δ_i of a drug transition moment is, in base-pair coordinates, $\delta_i' = \delta_i + \Delta$.

Using the Arnott convention (Arnott et al., 1969), we define a base pair long-axis Y', perpendicular to Z, along the N_1–C_4 axis of the 5′ pyrimidine in the drug complex. Next we define a positive X' axis, perpendicular to Y' and Z, facing into the small groove. The rotation of the intercalated drug axes relative to these base-pair axes can be measured directly from a projection of the complex down the Z axis. For example, $\Delta = 0$ if a drug is intercalated between base pairs such that its short axis X overlaps the short axis X' of its adjacent 5′ pyrimidine. Values of Δ are available in this way from X-ray diffraction (Jain et al., 1977; Tsai et al., 1977; Sobell & Jain, 1972; Neidel et al., 1977; Seshadri et al., 1977) and model building studies (Alden & Arnott, 1977).

After the base transition moment has been redefined in terms of the base coordinates (X', Y', and Z), eq 2 may be used to calculate, from the dichroism values ρ_i, the tilt θ_1' and twist θ_2' of the drug about the base-pair axes; if the drug and adjacent bases are parallel, the values θ_1' and θ_2' will also specify the tilt and twist of the adjacent bases. A calculation of θ_1' and θ_2' therefore specifies the angular orientation of the two base-pair piece of DNA adjacent to the drug.

These calculations are shown in Table II. Because in the available crystal structures EB, 9-AA, and AM are inter-

Table III

ligand	λ (nm)	method	lit. values ρ/ρ_{260}	lit. values α^a	exptl values ρ/ρ_{260}	exptl values α (deg)	λ (nm)	ligand
EB	520	ED[b,d]	0.818	69	0.73	67	520	EB
	320		0.727	68	0.68	70	320	
AM	440	FD[c,e]	0.50	63	0.52	63	440	AM
Acridine	502	ED[f]	1	73	1	73	365	9-AA
Orange	310		0.727	68	0.755	69	407	
PF	450	ED[g]	0.88	70	1.09	76	450	PF
quinacrine	455	FD[h]	0.96	72				

[a] Calculated assuming $\rho_\infty = -1.15$. [b] ED = electric dichroism. [c] FD = flow dichroism. [d] Houssier et al., 1974. [e] Gellert et al., 1965. [f] Houssier & Federicq, 1972. [g] Ramstein et al., 1973. [h] Lerman, 1963.

calated with X and Y axes rotated only a few degrees from the base-pair axes (Jain et al., 1977; Tsai et al., 1977; Sobell & Jain, 1972; Seshadri et al., 1977), the calculated tilt θ_1' and twist θ_2' of the two base pairs in the drug complex are identical with that of the intercalator. Drug and base-pair axes also overlap ($\Delta = 0$) in the proflavin–DNA complex proposed by Arnott (Alden & Arnott, 1977). Consequently the inclination of the drug is also identical with the inclination of adjacent base pairs. However, the proflavin–CpG crystal structure recently solved by Neidel et al. (1977) specifies an angle $\Delta = -27°$ between the two sets of axes. Because drug and base-pair axes do not overlap, the two sets of axes must be rotated differently to produce the measured drug orientation in the helix. The local proflavin–DNA geometry specified by the Neidel et al. crystal structure therefore predicts, from the measured dichroism and eq 2, values for θ_1' and θ_2' along base-pair axes which differ somewhat from the values θ_1 and θ_2 calculated for the drug axes. However, when calculated from the Neidel et al. geometry, the orientation of the two base pairs of DNA in the proflavin complex is very similar to the orientation calculated for DNA in the other drug complexes.

Discussion

These dichroism measurements have provided for the first time detailed information concerning the orientation of the intercalated drugs into DNA. Both flow and electric dichroism measurements have been made in the past for intercalators, but the studies have been limited to qualitative conclusions due to DNA polydispersity and the low, unknown degree of orientation attainable by flow or traditional electric dichroism techniques. In Table III we have compiled flow and electric dichroism measurements for DNA–intercalator complexes from several literature sources. Although the degree of orientation is unknown in these experiments, the studies cited in Table III did report the dichroism measured for DNA under their conditions. Since we have measured the dichroism of DNA at perfect orientation (-1.15 ± 0.1), the degree of orientation Φ attained in earlier studies may be calculated from the measured dichroism ρ_{obsd}, i.e., $\Phi = \rho_{obsd}/-1.15$. If we assume that the degree of orientation is unaffected by drug binding (which is not strictly true), approximate values for the dichroism angle α can be calculated using eq 1 from literature ρ values and Φ. In Table III we have presented these angles α, along with the measured ratio of drug dichroism values to that of uncomplexed DNA. In column 2 of Table III are, for comparison, the values α we have measured for intercalators, along with our drug–DNA dichroism ratios. As can be seen, when the published dichroism values are corrected for their unknown degree of orientation, they agree well with the values we have measured and, like our more accurate determinations of ρ, they imply that, when bound, intercalators are not perpendicular to the axes of orientation.

Conclusions

These dichroism measurements have provided three important kinds of information concerning the mechanism of intercalation.

First, the length increase which occurs upon intercalation is not exactly 3.4 Å for the four ligands tested, no doubt reflecting minor differences in the mechanism of intercalation.

Second, very little net bending or kinking of DNA is associated with intercalation. A 5° change in the average angle α due to bending, kinking, or superhelicity could have been detected, but was not.

Third and most importantly, this work argues very strongly that intercalated ligands are not perpendicular to the helix axis. The best generalization of the dichroism data for the four intercalators would be that the Y axis of the intercalated complex is tilted by $21 \pm 7°$ and the X or diad axis is twisted by $5 \pm 10°$. Such a tipped complex is substantially different from that predicted from dinucleotide crystal structures or from the energy minimization calculations which have been performed to calculate the preferred structure of intercalated complexes in B-form DNA.

The possibility exists that these differences reflect that inadequacy of either dinucleotide structures or the traditional B-form DNA structure as models for the structure of DNA in solution. As we discussed in an earlier paper (Hogan et al., 1978), our dichroism measurements and Levitt's energy minimization calculations (Levitt, 1978) suggest that in solution complementary bases in B DNA are not coplanar, each being propeller twisted with respect to the other by about 35° to give a DNA structure with an average base twist of 17°.

Extensive reversal of this twist would be necessary to maximize stacking interactions when a planar heterocycle intercalates between propellered base pairs. However, after flattening, planar base pairs would then be incompatible with adjacent regions of propellered DNA. Here, we explore the possibility that tilting is the mechanism by which the planar complex (the "complex" is the heterocycle plus the flat base pair on each side) is accommodated into DNA.

A model based upon intercalation between propeller-twisted DNA bases is presented in Figure 7. Part A is a schematic diagram of the DNA structure proposed by Levitt (1978) viewed from the DNA large groove. So viewed, the Levitt structure has bases tilted toward the 3′ direction, i.e., when facing the large groove, bases on the left strand twist with their nearer edge downward.

If, as has been proposed, the preferred site of intercalation is the symmetric helical segment 5′ py 3′–5′ pu, the distortions arising from loss of the propeller twist might express this same symmetry. Figure 7B is a hypothetical binding intermediate based upon a symmetric distortion of the complex. Because the intercalator is rigorously planar, the immediately adjacent

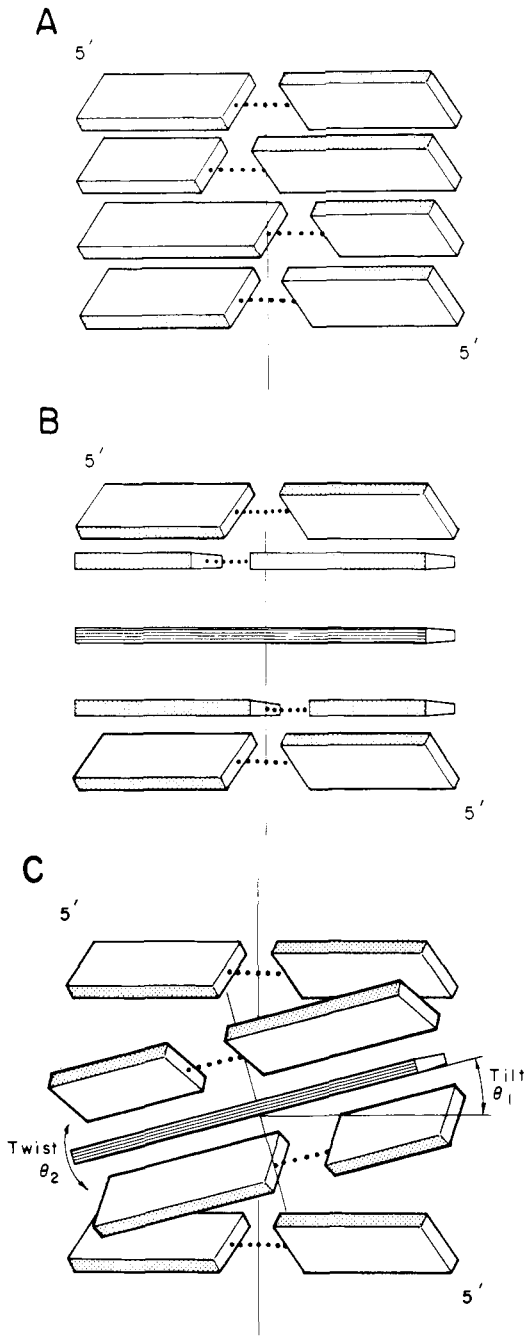

FIGURE 7: A model for intercalation into propeller-twisted DNA. (A) Schematic representation of the twisted DNA structure suggested by Levitt (1978). (B) Hypothetical binding intermediate which depicts the unfavorable contacts between flattened base pairs and adjacent propeller-twisted base pairs. (C) Model structure consistent with the dichroism data. Unfavorable contacts have been reduced by unstacking the 5′ pyrimidines. The complex is presented as being wedge shaped as viewed along the short base-pair axis to emphasize the variability seen for the twist of the complex. (See text for details.)

base pairs are forced to flatten. At the interface between these planar base pairs and propellered DNA, bases are no longer parallel, reducing base stacking and producing unfavorable contacts between bases.

We propose that relaxation from this structure may occur by increasing the separation between the 5′ py and its adjacent base. Since intercalated DNA is not kinked, the 17–28° measured tilt of the intercalated complex must be compensated at the interface. If this compensation occurs entirely by bending, as shown in Figure 7C, the 5′ py will be displaced from its 5′ neighbor, thereby reducing unfavorable contacts at the expense of pyrimidine base stacking. This compensating tilt is expected to contribute to the overall DNA length change but would vary with the amount of unwinding at the interface.

The intercalated complex also shows some twist of the diad axis, but the angle is small (~5°) and varies greatly among the four drugs. The gap which is produced at the 5′ py reduces unfavorable contacts but leaves adjacent bases nonparallel. Within the constraints of base pairing and stacking to the heterocycle, the 3′ pu could increase base stacking by twisting toward its 3′ neighbor (Figure 7C). This produces an intercalation site which is slightly wedge shaped, allowing for a small twist of the intercalator along X or perhaps a few degrees of conformational flexibility. Either alternative would have a similar effect on the dichroism.

References

Alden, C. J., & Arnott, S. (1977) *Proc. Natl. Acad. Sci. U.S.A. 2*, 1701–1717.

Arnott, S., Dover, S. D., & Wonacott, A. J. (1969) *Acta Crystallogr., Sect. B 25*, 2192.

Bresloff, J. (1974) Ph.D. Thesis, Yale University, New Haven, CT.

Broersma, S. (1960) *J. Chem. Phys. 32*, 1626–1631.

Cohen, G., & Eisenberg, H. (1969) *Biopolymers 8*, 45–55.

Crothers, D. M. (1968) *Biopolymers 6*, 575.

Crothers, D. M., Dattagupta, N., Hogan, M., Klevan, L., & Lee, K. S. (1978) *Biochemistry 17*, 4525–4533.

Dattagupta, N., Hogan, M., & Crothers, D. M. (1978) *Proc. Natl. Acad. Sci. U.S.A. 75*, 4286–4290.

Ding, D., Rill, R., & Van Holde, K. E. (1972) *Biopolymers 11*, 2109.

Dourlent, M., & Helene, C. (1971) *Eur. J. Biochem. 23*, 86–95.

Gellert, M., Smith, C. E., Neville, D., & Felsenfeld, G. (1965) *J. Mol. Biol. 11*, 445–457.

Hogan, M., Dattagupta, N., & Crothers, D. M. (1978) *Proc. Natl. Acad. Sci. U.S.A. 75*, 195–199.

Houssier, C., & Federicq, E. (1972) *Biopolymers 11*, 2281–2308.

Houssier, C., Hardy, B., & Fredericq, E. (1974) *Biopolymers 13*, 1141–1160.

Hudson, B., & Jacobs, B. (1975) *Biopolymers 14*, 1309–1312.

Ingram, L. L., & Johansen, H. (1969) *Arch. Biochem. Biophys. 132*, 205–209.

Jain, S. C., Tsai, C., & Sobell, H. M. (1977) *J. Mol. Biol. 114*, 317–331.

Klevan, L., Dattagupta, N., Hogan, M., & Crothers, D. M. (1978) *Biochemistry 17*, 4533–4540.

Krugh, T. R., & Reinhardt, C. G. (1975) *J. Mol. Biol. 97*, 133–162.

Lang, H., & Löber, G. (1969) *Tetrahedron Lett.* 4043–4047.

LePecq, J. B., & Paoletti, C. (1967) *J. Mol. Biol. 27*, 87–106.

Lerman, L. (1963) *Proc. Natl. Acad. Sci. U.S.A. 49*, 94–102.

Lerman, L. S., Luzzati, V., & Mason, F. (1961) *J. Mol. Biol. 3*, 634–639.

Levitt, M. (1978) *Proc. Natl. Acad. Sci., U.S.A. 75*, 640–644.

McGhee, J. D., & Von Hippel, P. H. (1974) *J. Mol. Biol. 86*, 469–489.

Müller, W., & Crothers, D. M. (1968) *J. Mol. Biol. 35*, 251–290.

Neidel, S., Achari, A., Taylor, G. L., Berman, H. M., Carrol, H. L., Glusker, J. P., & Stallings, W. C. (1977) *Nature (London) 269*, 304–307.

Okonski, C. T., Yoshioka, K., & Orttung, W. (1959) *J. Chem. Phys. 63*, 1558–1565.

Patel, D. J., & Canuel, L. L. (1977) *Biopolymers 16*, 857–873.

Ramstein, J., Houssier, C., & Leng, M. (1973) *Biochim. Biophys. Acta 335*, 54–68.
Rill, R. (1972) *Biopolymers 11*, 1929.
Sakore, T. D., Jahn, S. C., Tsai, C., & Sobell, H. (1977) *Proc. Natl. Acad. Sci., U.S.A. 74*, 188–192.
Scatchard, G. (1949) *Ann. N. Y. Acad. Sci. 51*, 660.
Seshadri, T., Sakore, T. D., & Sobell, H. M. (1977) American Crystallography Association Abstract No. 2, N5.
Sobell, H., & Jain, S. C. (1972) *J. Mol. Biol. 68*, 21–34.
Tinoco, I. (1955) *J. Am. Chem. Soc. 77*, 4486.
Tsai, C., Jain, S. C., & Sobell, H. M. (1977) *J. Mol. Biol. 114*, 301–315.
Turro, N. J. (1965) *Molecular Photochemistry*, W. A. Benjamin, New York.
Waring, M. (1965) *J. Mol. Biol. 13*, 269–282.
Weill, G., & Calvin, M. (1963) *Biopolymers 1*, 401–417.
Wittwer, A., & Zanker, V. (1959) *Z. Phys. Chem. (Frankfurt am Main) 22*, 417–439.
Yamoka, K., & Ziffer, H. (1968) *Biochemistry 7*, 1001–1008.
Zanker, V., & Schmid, W. (1957) *Chem. Ber. 3*, 2253–2265.
Zanker, V., & Wittner, A. (1963) *Z. Phys. Chem. (Frankfurt am Main) 24*, 183–205.
Zipper, P., & Bünemann, H. (1975) *Eur. J. Biochem. 51*, 3–17.

Determining Globular Protein Stability: Guanidine Hydrochloride Denaturation of Myoglobin†

C. Nick Pace* and Keith E. Vanderburg

ABSTRACT: The guanidine hydrochloride (Gdn·HCl) denaturation of horse myoglobin has been investigated at several pH values using absorbancy measurements at 409 nm. From these data the free energy of denaturation, ΔG_D, can be calculated and ΔG_D values have been measured to zero concentrations of denaturant. The dependence of ΔG_D on Gdn·HCl concentration, $d(\Delta G_D)/d(\text{Gdn·HCl})$, increases markedly as the denaturant concentration decreases. This indicates that an increase in the number of Gdn·HCl binding sites on unfolding is the major driving force for denaturation by Gdn·HCl. An equation based on denaturant binding which fits the experimental data for myoglobin at pH 7 is $\Delta G_D = \Delta G_D^{H_2O} - \Delta nRT \ln (1 + ka_\pm)$, where $\Delta G_D^{H_2O}$ (= 10.1 kcal/mol) is the free energy of denaturation in the absence of denaturant, Δn (= 42.8) is the difference in the number of Gdn·HCl binding sites on the native and denatured states of the protein, k (= 0.6) is the average denaturant binding constant, and $a_\pm$ is the mean ion activity of Gdn·HCl. Several lines of evidence are presented which show convincingly that $k = 0.6$ should be used in the analysis of Gdn·HCl denaturation curves rather than $k = 1.2$ which is currently in widespread use. In addition, for myoglobin and four other proteins, an equivalent and more convenient method of analyzing Gdn·HCl denaturation curves is to use Gdn·HCl molarities rather than mean ion activities and a denaturant binding constant of 0.8.

Guanidine hydrochloride (Gdn·HCl),[1] urea, and sodium dodecyl sulfate are the three most popular protein denaturants. Gdn·HCl and urea produce a randomly coiled denatured state (Tanford, 1968) which, for many purposes, is a more useful denatured state than the helical, rod-like denatured state (Reynolds & Tanford, 1970) produced by sodium dodecyl sulfate. The use of Gdn·HCl as a denaturant has increased substantially over the past 10 years. Gdn·HCl is a more potent denaturant than urea, unfolding proteins at two to three times lower concentrations (Greene & Pace, 1974), and Gdn·HCl is chemically stable, while urea slowly decomposes to form cyanate and ammonia.

One of the interesting results from a study of the Gdn·HCl denaturation of a globular protein is an estimate of the stability of the protein; i.e., it is possible to estimate the free energy change, ΔG_D, for the reaction, globular conformation $\rightleftharpoons$ randomly coiled conformation, in the absence of denaturant, $\Delta G_D^{H_2O}$. This is done by measuring ΔG_D as a function of Gdn·HCl concentration and extrapolating to zero concentration. Several different approaches have been used for making this extrapolation, but, unfortunately, they lead to estimates of $\Delta G_D^{H_2O}$ which differ by as much as 20–50%. Thus it has been possible to show that the stability of globular proteins is remarkably low, but it has not been possible to determine with certainty small differences in stability between, for example, homologous proteins or chemically modified proteins (Pace, 1975).

Aune & Tanford (1969) made the first serious attempt to estimate $\Delta G_D^{H_2O}$ using data from a Gdn·HCl denaturation study. They state that the fact that Gdn·HCl promotes unfolding "... requires that more guanidinium and/or chloride ions are bound to the denatured form than to the native form; or that more water is bound to the native form than to the denatured forms; or a combination of these effects." They showed that several different models for analyzing denaturization in terms of binding were consistent with their data and could not be distinguished. The model used subsequently by Tanford's laboratory (Salahuddin & Tanford, 1970) and many other groups (Pace, 1975; Ahmad & Salahuddin, 1976; McLendon & Sandburg, 1978; Ahmad & McPhie, 1978) ignored the contribution of changes in water binding (Tanford, 1970) and assumed that denaturation results from an increase in the number of binding sites for guanidinium ions on unfolding. This model led to an equation of the form:

$$\Delta G_D = \Delta G_D^{H_2O} - \Delta nRT \ln (1 + ka_\pm) \quad (1)$$

† From the Department of Biochemistry & Biophysics, Texas A&M University, and the Texas Agricultural Experiment Station, College Station, Texas 77843. *Received February 8, 1978; revised manuscript received June 6, 1978.*

[1] Abbreviation used: Gdn·HCl, guanidine hydrochloride.

0006-2960/79/0418-0288$01.00/0